(45.4 mg, 0.20 mmol). Stirring for 0.5 h was followed by concentration to ca. 2 mL and then addition of petroleum ether. The yellow powder that precipitated was collected and recrystallized from $CHCl_3/CH_3OH$ (115 mg, 95%). Microanalytical data for the complexes are shown in Table VI.

Preparation of *trans*-$PtCl_2$(4)(C_2H_4). [Pt(μ-Cl)Cl(C_2H_4)]$_2$ (59 mg, 0.10 mmol) was suspended in 10 mL of CH_2Cl_2 and then treated with **4** (27 μL, 29 mg, 0.20 mmol). Stirring at room temperature was followed by concentration to ca. 2 mL. Addition of petroleum ether induced precipitation of the product, which was recrystallized from CH_2Cl_2/hexane to afford 83 mg (94%) of pure complex.

Crystallography. White air-stable crystals of *trans*-$PtCl_2$(**5**)(PEt_3) suitable for X-ray diffraction were obtained via recrystallization from CH_2Cl_2/hexane. A crystal of prismatic habit was mounted on a glass fiber at a random orientation. The determination of lattice parameters and space group and the data collection were carried out on a Enraf-Nonius CAD4 diffractometer. Cell constants were obtained by a least-squares fit of the 2θ values of 25 high-angle reflections using the CAD4 centering routines. Crystallographic and data collection parameters are listed in Table IV and in Table S1. Data were collected at variable scan speed to obtain constant statistical precision on the recorded intensities.

Three standard reflections ($1\bar{4}\bar{3}$, $0\bar{3}\bar{4}$, $\bar{1}43$) were measured every hour to monitor the stability of the crystal, while the orientation was checked every 300 reflections by measuring three standards (344, $03\bar{6}$, $\bar{3}\bar{4}4$). No significant variations were detected. Data were corrected for Lorentz and polarization factors[38] and an empirical absorption correction was applied using azimuthal (Ψ) scans of three reflections at high χ angles ($85.4 \leq \chi \leq 87.2°$) by using the SDP crystallographic programs.[39] The standard deviations on intensities were calculated in terms of statistics alone, while those on F_o were calculated according to the formula $\sigma(F_o) = [\sigma^2(F_o^2) + f^2(F_o^2)]^{1/2}/2F_o$ with $f = 0.040$. An $F_o = 0.0$ value was given to those reflections having negative net intensities. The structure was solved by Patterson and Fourier methods and refined by full-matrix least-squares techniques. The function minimized was $\sum w(|F_o| - (1/k)|F_c|)^2$ with $w = [\sigma^2(F_o)]^{-1}$. Anisotropic thermal parameters were used for all atoms. Although peaks (ca. 0.7–0.8 e/Å^3) could be found in the final Fourier difference map corresponding to most of the hydrogen atoms, only their contribution in calculated positions (C–H = 0.95 Å, B_{iso} = 5.0 Å^2) was taken into account but not refined with the exception of the structurally significative H(10), which was located and refined. Final coordinates and equivalent thermal factors are given in Table V. Scattering factors were taken from the literature,[40] and the contribution of the real and imaginary part of the anomalous dispersion was taken into account.[38] No extinction correction was deemed necessary. All calculations were carried out by using the SDP crystallographic package.

Acknowledgment. A.A. thanks MPI and P.S.P. thanks the ETH Zürich and the Swiss National Science Foundation for support and the Johnson Matthey Research Centre, England, for the loan of platinum metals.

Supplementary Material Available: Tables of X-ray experimental data, hydrogen coordinates, anisotropic thermal factors, and extended bond lengths and angles (8 pages); a table of observed and calculated structure factors (33 pages). Ordering information is given on any current masthead page.

---

(38) Arndt, U. V.; Willis, B. T. M. *Single Crystal Diffractometry*; Cambridge University Press: Cambridge, England, 1966.

(39) *Enraf-Nonius Structure Determination Package SDP*; Enraf-Nonius: Delft, The Netherlands, 1987.

(40) *International Tables for X-ray Crystallography*; Kynoch Press: Birmingham, England, 1974; Vol. IV.

Contribution from the Laboratoire de Synthèse et d'Electrosynthèse Organométalliques associé au CNRS (URA 33),
Faculté des Sciences, Université de Bourgogne, 6 bd Gabriel, 21000 Dijon, France, and Laboratoire de Chimie des Métaux
de Transition associé au CNRS (UA 419), Université P. et M. Curie, 75252 Paris Cédex 05, France

[1]Ferrocenophanes Containing a Group 4 Transition Metal in the Bridge. X-ray Structure of One Representative

Roland Broussier,[1a] Anne Da Rold,[1a] Bernard Gautheron,*,[1a] Yves Dromzee,[1b] and Yves Jeannin[1b]

Received May 31, 1989

New [1]ferrocenophanes (RC_5H_4)$_2$ML_2 (**1**) (R = H, *t*-Bu; L_2 = (C_5H_4)$_2$Fe; M = Ti, Zr, Hf) containing a transition metal in the "phane" bridge have been obtained when the 1,1'-dilithioferrocene–TMEDA complex was reacted with metallocene dichloride at room temperature. Compounds **1** exposed to air led to μ-oxo complexes [(C_5H_5)$_2$ML']$_2$O (L' = (C_5H_5)(C_5H_4)Fe). Spectroscopically speaking, the ferrocene part of the molecules is the most affected by structural strains and by the bridging metal electronegativity. The molecular structure of [(H_3C)$_3$CC_5H_4]$_2$Zr(C_5H_4)$_2$Fe has been determined by a single-crystal X-ray diffraction study. The crystal was found to be monoclinic, *C*2/*c*, with *a* = 18.715 (2) Å, *b* = 9.691 (1) Å, *c* = 14.923 (2) Å, β = 122.47 (1)°, *V* = 2283 (1) Å^3, and *Z* = 4. The structure was refined to *R* = 0.026 and R_w = 0.029 with use of 2685 unique reflections with $I \geqslant 3\sigma(I)$ recorded at room temperature. The Zr–Fe distance equal to 2.9621 (5) Å might suggest the occurrence of a weak dative bond between electron-rich and electron-poor metal centers.

Introduction

Many papers dealing with [*n*]ferrocenophanes emphasize the potential ability of the bridging chain to induce steric and electronic perturbations at the iron atom.[2-5] If *n* is small, these effects can result from the bulkiness of the cyclopentadienyl ligands, while greater *n* values allow direct interactions between the iron atom and part of the flexible bridging chain. With the hope of finding both effects in the same molecule, we have now prepared ferrocenophanes incorporating a group 4 transition metal in a short bridge. These new molecules contain one electron-rich and one electron-poor metallic center capable of synergistic interactions. We now report the synthesis and spectroscopic properties of some metalla[1]ferrocenophanes (M = Ti, Zr, Hf), together with the X-ray structure of a representative example, (*t*-BuC_5H_4)$_2$ZrL_2 (L_2 = (C_5H_4)$_2$Fe).

Experimental Section

Materials and Instrumentation. All reactions were conducted under an argon atmosphere with Schlenk tube techniques. Solvents were dried and deoxygenated over sodium/benzophenone ketyl and distilled just before use (transfers were carried out via syringes or cannulas). Melting

---

(1) (a) Université de Bourgogne. (b) Université P. et M. Curie.

(2) Czech, B.; Piorko, A.; Annunziata, R. *J. Organomet. Chem.* **1983**, *255*, 365.

(3) Orrell, K. G.; Sik, V.; Brubaker, C. H.; McCulloch, B. *J. Organomet. Chem.* **1984**, *276*, 267 and references therein.

(4) Sato, M.; Tanaka, S.; Ebine, S.; Morinaga, K.; Akabori, S. *J. Organomet. Chem.* **1985**, *282*, 247.

(5) Sato, M.; Sekino, M.; Akabori, S. *J. Organomet. Chem.* **1988**, *344*, C31.

0020-1669/90/1329-1817$02.50/0

points were determined with a Kofler apparatus. ^1H and ^{13}C nuclear magnetic resonance spectra were recorded on a JEOL FX 100 spectrometer. Chemical shifts are reported in δ units, parts per million downfield from internal tetramethylsilane. Mass spectra were obtained by using a Finnigan type 3300 spectrometer operating at 70 eV; results are given as m/e for main fragments (relative intensity: ^{48}Ti, ^{56}Fe, ^{90}Zr, ^{180}Hf). Electronic and visible spectra were recorded on a Perkin-Elmer 559 instrument in argon-purged 10-mm cells (solution in hexane). Microanalyses were obtained from the Service Central d'Analyses du CNRS.

(1,1′-Ferrocenediyl)titanocene: **$(C_5H_5)_2TiL_2$, $L_2 = (C_5H_4)_2Fe$.** A solution of $Fe(C_5H_4Li)_2 \cdot TMEDA$[6] (0.79 g, 2.5 mmol) in THF (20 mL) was added to a stirred suspension of $(C_5H_5)_2TiCl_2$ (0.63 g, 2.5 mmol) in THF (20 mL). Stirring was maintained at 25 °C for 12 h, and the solvent was eliminated under reduced pressure. The solid residue was recrystallized from toluene. The brown crystals were washed twice with cold toluene and dried (0.3 g, 0.83 mmol, 33%): mp 241 °C; mass spectrum 362 (M^+, 72), 296 ($M^+ - C_5H_6$, 42), 250 ($M^+ - TiC_5H_4$, 43), 186 ($C_{10}H_{10}Fe^+$, 100), 121 ($C_5H_5Fe^+$, 47). Anal. Calcd for $C_{20}H_{18}FeTi$: C, 66.19; H, 5.08. Found: C, 66.42; H, 5.11.

(1,1′-Ferrocenediyl)zirconocene: **$(C_5H_5)_2ZrL_2$, $L_2 = (C_5H_4)_2Fe$.** A solution of $(C_5H_5)_2ZrCl_2$ (1.1 g, 3.78 mmol) in a mixture of toluene/THF (1/1, 20 mL) was slowly added at 25 °C to a stirred solution of $Fe(C_5H_4Li)_2 \cdot TMEDA$ (1.19 g, 3.78 mmol) in the same solvent (20 mL). After 2 h of stirring, the solid was filtered and recrystallized from toluene, yielding 0.47 g (1.16 mmol, 31%) of very air-sensitive deep yellow crystals: mass spectrum 404 (M^+, 15), 339 ($M^+ - C_5H_5$, 40), 186 ($C_{10}H_{10}Fe^+$, 100), 121 ($C_5H_5Fe^+$, 52).

(1,1′-Ferrocenediyl)hafnocene: **$(C_5H_5)_2HfL_2$, $L_2 = (C_5H_4)_2Fe$.** By use of the same experimental process as above, $(C_5H_5)_2HfCl_2$ (0.7 g, 1.85 mmol) and $Fe(C_5H_4Li)_2 \cdot TMEDA$ (0.58 g, 1.85 mmol) afforded 0.27 g (0.55 mmol, 30%) of very air-sensitive light orange crystals: mass spectrum 494 (M^+, 80), 492 ($M^+ - H_2$, 100), 427 ($M^+ - H_2 - C_5H_5$, 26), 371 ($M^+ - H_2–C_5H_5Fe$, 28), 347 ($C_{10}H_8HfC_3H_3^+$, 28), 186 ($C_{10}H_{10}Fe^+$, 21), 121 ($C_5H_5Fe^+$, 37).

(1,1′-Ferrocenediyl)di-*tert*-butyltitanocene: **$(t\text{-}BuC_5H_4)_2TiL_2$, $L_2 = (C_5H_4)_2Fe$.** The experimental conditions were those used for the unsubstituted derivative except that the solvent was the mixture toluene/THF (1/1). The reaction led to brown crystals (45%) from heptane: mp 213 °C; ^{13}C NMR (C_6D_6) δ C 33.2 (C(7–9)), 71.5–86.0 (C(12–15)), 104.8 (C(2,3)), 106.4 (C(1,4)), 137.6 (C(5)), 179.8 (C(11)); mass spectrum 474 (M^+, 68), 353 ($M^+ - t\text{-}BuC_5H_4$, 21), 337 ($M^+ - CH_4 - t\text{-}BuC_5H_4$, 64), 186 ($C_{10}H_{10}Fe^+$, 100), 121 ($t\text{-}BuC_5H_4^+$ and $C_5H_5Fe^+$, 67), 107 ($C_8H_{11}^+$, 58), 91 ($C_7H_7^+$, 45). Anal. Calcd for $C_{28}H_{34}FeTi$: C, 70.9; H, 7.22. Found: C, 70.21; H, 7.33.

(1,1′-Ferrocenediyl)di-*tert*-butylzirconocene: **$(t\text{-}BuC_5H_4)_2ZrL_2$, $L_2 = (C_5H_4)_2Fe$.** The procedure was that used for the unsubstituted compound, but the reaction time was 12 h. The final recrystallization (heptane) yielded deep orange crystals (50%): mp 221 °C; ^{13}C NMR (C_6D_6) δ C 33.2 (C(7–9)), 70.8–83.5 (C(12–15)), 105.2 (C(1–4)), 138.6 (C(5)), 159.0 (C(11)); mass spectrum 516 (M^+, 14), 379 ($M^+ - CH_4 - t\text{-}BuC_5H_4$, 6), 274 ($M^+ - 2t\text{-}BuC_5H_4$, 36), 186 ($C_{10}H_{10}Fe^+$, 85), 121 ($t\text{-}BuC_5H_4^+$ and $C_5H_5Fe^+$, 89), 107 ($C_8H_{11}^+$, 67), 91 ($C_7H_7^+$, 100). Anal. Calcd for $C_{28}H_{34}FeZr$: C, 64.97; H, 6.62; Zr, 17.62; Fe, 10.79. Found: C, 64.33; H, 6.62; Zr, 18.88; Fe, 10.10.

(1,1′-Ferrocenediyl)di-*tert*-butylhafnocene: **$(t\text{-}BuC_5H_4)_2HfL_2$, $L_2 = (C_5H_4)_2Fe$.** Following the same experimental procedure as for the isologue zirconocene, the reaction afforded orange crystals (36%) from heptane: mp 231 °C dec; ^{13}C NMR (C_6D_6) δ C 33.2 (C(7–9)), 71.8–84.0 (C(12–15)), 104.6 (C(1–4)), 137.5 (C(5)), 153.3 (C(11)); mass spectrum 606 (M^+, 94), 604 ($M^+ - H_2$, 10), 469 ($M^+ - CH_4 - t\text{-}BuC_5H_4$, 24), 467 ($M^+ - H_2–CH_4 - t\text{-}BuC_5H_4$, 33), 429 ($M^+ - t\text{-}BuC_5H_4 - Fe$, 20), 427 ($M^+ - H_2 - t\text{-}BuC_5H_4 - Fe$, 38), 364 ($M^+ - 2t\text{-}BuC_5H_4$, 58), 186 ($C_{10}H_{10}Fe^+$, 58), 121 ($t\text{-}BuC_5H_4^+$ and $C_5H_5Fe^+$, 36), 107 ($C_8H_{11}^+$, 25), 91 ($C_7H_7^+$, 32). Anal. Calcd for $C_{28}H_{34}FeHf$: C, 55.60; H, 5.66; Hf, 29.51; Fe, 9.25. Found: C, 56.40; H, 5.74; Hf, 29.75; Fe, 9.24.

(μ-Oxo)bis(ferrocenylzirconocene): **$[(C_5H_5)_2ZrL']_2O$, $L' = (C_5H_5)(C_5H_4)Fe$.** This complex was obtained directly from solid $(C_5H_5)_2Zr(C_5H_4)_2Fe$ (0.5 g, 1.24 mmol) exposed to the atmosphere for 5 h. Recrystallization of the product from toluene afforded golden yellow crystals (0.30 g, 0.35 mmol, 28%): mp > 260 °C; ^1H NMR ($CDCl_3$) δ 5.98 (s, 10), 4.35 (m, 2), 4.22 (m, 2), 4.04 (s, 5); mass spectrum 826 (M^+, 50), 641 ($M^+ - C_{10}H_9Fe$, 13), 576 ($M^+ - C_5H_5 - C_{10}H_9Fe$, 63), 456 ($M^+ - 2C_{10}H_9Fe$, 86), 391 ($M^+ - C_5H_5 - 2C_{10}H_9Fe$, 100), 186 ($C_{10}H_{10}Fe^+$, 92). Anal. Calcd for $C_{40}H_{38}Fe_2Zr_2O$: C, 57.96; H, 4.62. Found: C, 58.10; H, 4.55.

Table I. Crystal Data

formula	$FeZrC_{28}H_{34}$	Z	4
fw	517.6	ρ_{calcd}, g cm^{-3}	1.51
space group	$C2/c$	T, °C	20
a, Å	18.715 (2)	λ, Å	0.71069
b, Å	9.691 (1)	μ(Mo Kα), cm^{-1}	10.97
c, Å	14.923 (2)	$R = R(F_o)$	0.026
β, deg	122.47 (1)	$R_w = R_w(F_o)$	0.029
V, Å^3	2.283		

Table II. Fractional Atomic Coordinates with Estimated Standard Deviations in Parentheses

atom	x/a	y/b	z/c	U_{iso},[a] Å^2
Zr(1)	0.0000	0.06025 (2)	0.2500	0.0243
Fe(1)	0.0000	0.36590 (4)	0.2500	0.0421
C(1)	−0.1431 (1)	0.0571 (3)	0.0698 (1)	0.0401
C(2)	−0.0794 (1)	0.0116 (3)	0.0531 (1)	0.0443
C(3)	−0.0487 (1)	−0.1129 (3)	0.1051 (2)	0.0431
C(4)	−0.0932 (1)	−0.1466 (2)	0.1539 (2)	0.0404
C(5)	−0.15317 (9)	−0.0422 (2)	0.1316 (1)	0.0336
C(6)	−0.2225 (1)	−0.0521 (2)	0.1559 (1)	0.0363
C(7)	−0.2782 (2)	0.0746 (3)	0.1197 (3)	0.0602
C(8)	−0.1849 (1)	−0.0704 (4)	0.2745 (2)	0.0568
C(9)	−0.2772 (2)	−0.1782 (4)	0.0988 (3)	0.0613
C(11)	0.0566 (1)	0.2322 (2)	0.2023 (2)	0.0366
C(12)	−0.0020 (2)	0.3218 (3)	0.1150 (2)	0.0500
C(13)	0.0206 (2)	0.4618 (3)	0.1423 (4)	0.0616
C(14)	0.0947 (2)	0.4657 (2)	0.2446 (4)	0.0573
C(15)	0.1177 (1)	0.3278 (2)	0.2811 (2)	0.0455

[a] $U_{iso} = (U_1U_2U_3)^{1/3}$.

(μ-Oxo)bis(ferrocenylhafnocene): **$[(C_5H_5)_2HfL']_2O$, $L' = (C_5H_5)(C_5H_4)Fe$.** Exposed for 3 h to air, 0.5 g (1 mmol) of solid $(C_5H_5)_2Hf(C_5H_4)_2Fe$ led to golden yellow crystals recrystallized from toluene (0.27 g, 0.27 mmol, 27%): mp > 260 °C; ^1H NMR ($CDCl_3$) δ 5.93 (s, 10), 4.36 (t, 2), 4.24 (t, 2), 4.04 (s, 5); mass spectrum 755 ($M^+ - C_5H_5 - C_{10}H_{10}Fe$, 3), 754 ($M^+ - C_5H_6 - C_{10}H_{10}Fe$, 5), 689 ($M^+ - C_5H_5 - C_5H_6 - C_{10}H_{10}Fe$, 4), 688 ($M^+ - 2C_5H_6 - C_{10}H_{10}Fe$, 6), 635 ($M^+ - C_{10}H_9Fe - C_{10}H_{10}Fe$, 4), 634 ($M^+ - 2C_{10}H_{10}Fe$, 6), 570 ($M^+ - C_5H_5 - C_{10}H_9Fe–C_{10}H_{10}Fe$, 3), 569 ($M^+ - C_5H_5 - 2C_{10}H_{10}Fe$, 8), 250 ($C_{15}H_{14}Fe^+$, 23), 186 ($C_{10}H_{10}Fe^+$, 100), 121 ($C_5H_5Fe^+$, 53). Anal. Calcd for $C_{40}H_{38}Fe_2Hf_2O$: C, 47.88; H, 3.82; Hf, 35.58. Found: C, 47.81; H, 3.75; Hf, 34.96.

Crystal Structure Determination for $(t\text{-}BuC_5H_4)_2ZrL_2$, $L_2 = (C_5H_4)_2Fe$. A single crystal measuring 0.5 × 0.5 × 0.3 mm was sealed under argon in a thin-walled glass capillary. Preliminary Laue and precession photographs led to a monoclinic unit cell. The observed systematic absences for $|hkl|$ and for $|h0l|$ are compatible with both space groups Cc and $C2/c$. The centrosymmetric space group was chosen on the basis of statistical tests and confirmed by subsequent results. Four molecules per unit cell imply that some atoms lie on special positions. Each molecule lies along a 2-fold axis on which zirconium and iron atoms are located.

Diffraction measurements were carried out on a four-circle CAD-4 diffractometer. Unit cells were determined and refined from 25 randomly selected reflections.

Crystal data, data collection parameters, and refinement residuals are given in Table I. During intensity data collection two standard reflections were measured periodically and showed no apparent intensity variation. Recorded intensities were corrected for Lorentz–polarization effects. Absorption corrections were then applied on the basis of scan curves via an empirical technique.[7] Reflections with $I \leqslant 3\sigma(I)$ were declared unobserved and excluded from subsequent calculations.

Structural Determination and Refinement. Computations were performed by using the CRYSTALS[8] package system adapted for a MicroVAX computer.

The positions of the two independent heavy atoms were deduced from a Patterson map. All other non-hydrogen atoms were found on successive difference Fourier maps. All the hydrogen atoms were located on a

---

(6) Bishop, J. J.; Davison, A.; Katcher, M. L.; Lichtenberg, D. W.; Merrill, R. E.; Smart, J. C. *J. Organomet. Chem.* **1971**, *27*, 241.

(7) North, A. C. T.; Philipps, D. C.; Mathews, F. S. *Acta Crystallogr., Sect. A: Cryst. Phys. Diffr., Theor. Gen. Crystallogr.* **1968**, *A24*, 351.

(8) Carruthers, J. R.; Watkin, D. J. *CRYSTALS*; Chemical Crystallography Laboratory, University of Oxford: Oxford, England, 1986.

(9) Prince, E. *Mathematical Techniques in Crystallography*; Springer-Verlag, Berlin, 1982.

(10) Seyferth, D.; Withers, H. *J. Organomet. Chem.* **1980**, *185*, C1.

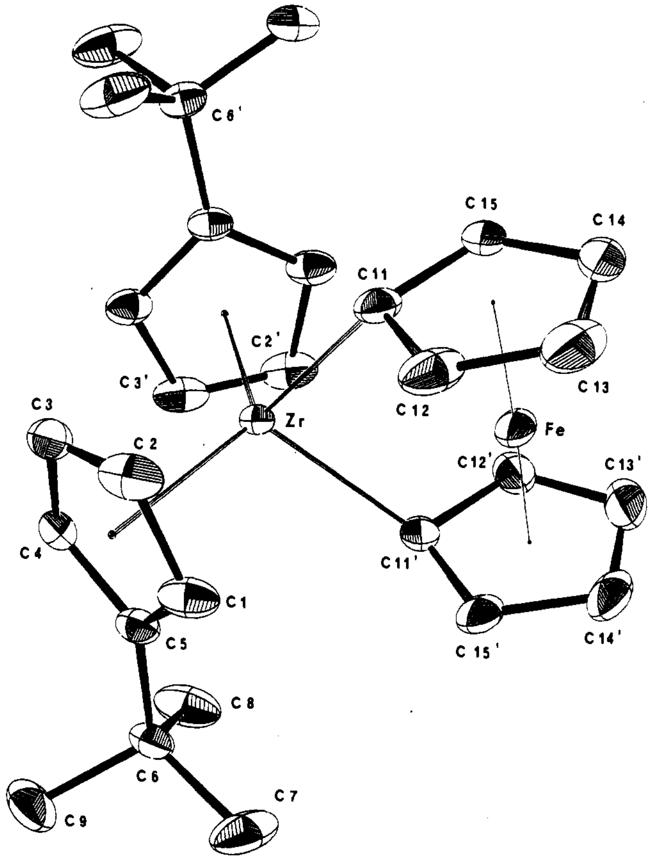

Figure 1. ORTEP view of the Cp'_2ZrCp_2Fe molecule, showing the atom numbering used in the tables.

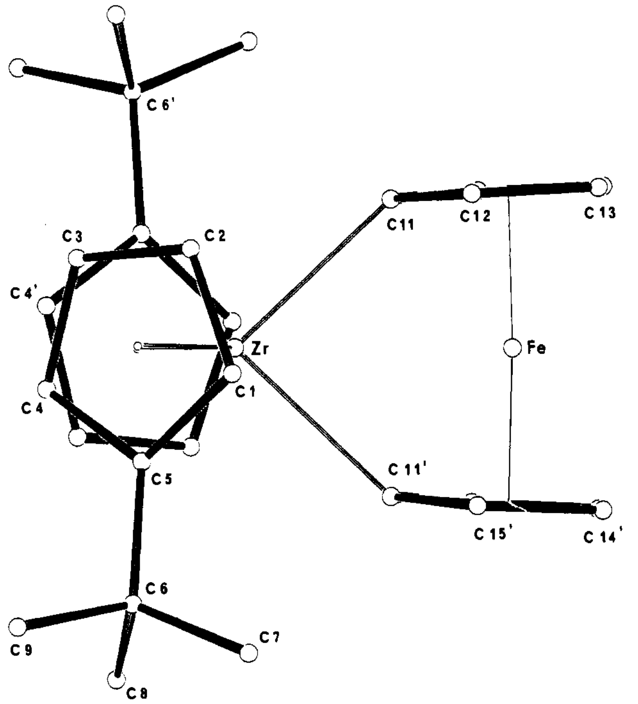

Figure 2. Projection onto the plane defined by atoms Zr, C_{11}, and C_{11}'.

difference electron density map. All the non-hydrogen atoms were refined with anisotropic thermal parameters, and all hydrogen atoms, with one common variable isotropic thermal parameter. The final least-squares calculation converged with residuals as given in Table I. A final difference map showed no residual electron density greater than 0.4 e $Å^{-3}$. Final atomic coordinates are listed in Table II. Selected bond distances and angles are given in Table III. The molecular geometry and the atom numbering are shown in Figures 1 and 2. Tables containing additional distances and angles, the positions of hydrogen atoms, thermal parameters, and structure factors are available as supplementary material.

Table III. Bond Lengths (Å) and Angles (deg) with Estimated Standard Deviations in Parentheses[a-e]

Zr–Fe	2.9621 (5)	Cp(11)–Zr–Cp(11′)	86.3 (1)
Zr–C(11)	2.284 (2)	Cp′(c)–Zr–Cp′(c′)	125.31 (6)
Zr–Cp′	2.2549 (9)	Cp′(c)–Zr–C(11)	109.31 (6)
Zr–C(1)	2.583 (2)	Cp′(c)–Zr–C(11′)	109.85 (5)
Zr–C(2)	2.525 (2)	Cp′(c)–Zr–Fe	117.34 (3)
Zr–C(3)	2.492 (2)		
Zr–C(4)	2.536 (2)	Cp(c)–Fe–Cp(c′)	177.27 (8)
Zr–C(5)	2.624 (2)		
Zr–C(av)	2.55 (5)	C(5)–C(1)–C(2)	108.8 (2)
		C(1)–C(2)–C(3)	108.1 (2)
Fe–Cp	1.642 (2)	C(2)–C(3)–C(4)	108.0 (2)
Fe–C(11)	2.029 (2)	C(3)–C(4)–C(5)	109.1 (2)
Fe–C(12)	2.041 (3)	C(4)–C(5)–C(1)	105.9 (2)
Fe–C(13)	2.064 (3)	C(4)–C(5)–C(6)	124.6 (2)
Fe–C(14)	2.059 (2)	C(5)–C(6)–C(7)	112.0 (2)
Fe–C(15)	2.027 (2)	C(5)–C(6)–C(8)	111.2 (1)
Fe–C(av)	2.04 (2)	C(5)–C(6)–C(9)	108.6 (2)
		C(7)–C(6)–C(8)	108.0 (2)
C(1)–C(2)	1.413 (3)	C(7)–C(6)–C(9)	108.9 (2)
C(2)–C(3)	1.381 (4)	C(8)–C(6)–C(9)	108.0 (2)
C(3)–C(4)	1.409 (3)		
C(4)–C(5)	1.412 (3)	C(12)–C(11)–C(15)	103.4 (2)
C(1)–C(5)	1.413 (3)	C(11)–C(12)–C(13)	110.4 (3)
C(5)–C(6)	1.527 (2)	C(12)–C(13)–C(14)	107.9 (2)
C(6)–C(7)	1.511 (3)	C(13)–C(14)–C(15)	108.0 (3)
C(6)–C(8)	1.523 (3)	C(11)–C(15)–C(14)	110.3 (3)
C(6)–C(9)	1.526 (3)		
C(11)–C(12)	1.456 (3)		
C(12)–C(13)	1.415 (4)		
C(13)–C(14)	1.408 (6)		
C(14)–C(15)	1.420 (4)		
C(15)–C(11)	1.451 (3)		

[a] Cp denotes the cyclopentadienyl ring C_5H_5 of the iron moiety. [b] Cp′ denotes the cyclopentadienyl ring t-BuC_5H_4 of the zirconium moiety. [c] Cp(c) refers to the centroid of the cyclopentadienyl ring. [d] A prime refers to the equivalent position relative to the x, y, z set: $-x$, y, $0.5 - z$. [e] (av) means the standard deviation for the averaged values is taken as the larger of $[\sum_{i=1}^{i=n}(x_i - x)^2/n(n-1)]^{1/2}$ and $[(\sum_{i=1}^{i=n}\sigma_i^2)^{1/2}]/n$ where x_i and σ_i are the individual observations and their esd's, respectively.

Results and Discussion

Among the [*n*]ferrocenophanes, the number of [1]ferrocenophanes is very limited, and all contain elements of groups 14 (Si, Ge) and 15 (P, As),[11-14] for which the ionic radius is smaller than that of the transition metals studied in the present work. Several attempts to synthesize ferrocenophanes containing a tin atom in the bridge led to a polymeric material[11,13] from which dimeric compounds were isolated. These dimers can be formulated with one tin atom bonded to two ferrocene moieties.[13]

Unprecedented metalla[1]ferrocenophanes (**1**) were prepared by reaction 1, already used for other [1]ferrocenophane syntheses.

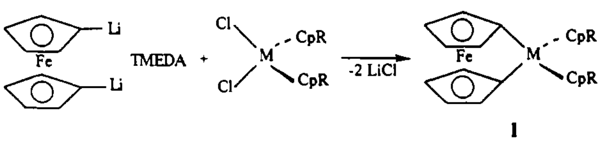

1

R = H, t-Bu; M = Ti, Zr, Hf (1)

The procedure involves reaction of 1,1′-dilithioferrocene–tetramethylenediamine[6] with a convenient metallocene dichloride at room temperature. This allowed the successful preparation of (1,1′-ferrocenediyl)dicyclopentadienyl- or 1,1′-ferrocenediyl)bis(*tert*-butylcyclopentadienyl)titanium, -zirconium, and -hafnium.

---

(11) Osborne, A. G.; Whiteley, R. H.; Medas, R. E. *J. Organomet. Chem.* **1980**, *193*, 345.

(12) Stoeckli-Evans, H.; Osborne, A. G.; Whiteley, R. H. *J. Organomet. Chem.* **1980**, *194*, 91.

(13) Seyferth, D.; Withers, H. *Organometallics* **1982**, *1*, 1275.

(14) Butler, I. R.; Cullen, W. R.; Beinstein, F. W.; Rettig, S.; Willis, A. J. *Organometallics* **1983**, *2*, 128.

Table IV. ^1H NMR Data (ppm) for [1]Ferrocenophanes[a,b]

			$(t\text{-}BuC_5H_4)_2M(C_5H_4)_2Fe$				$(C_5H_5)_2M(C_5H_4)_2Fe$		
M		*t*-Bu	$(C_5H_4)_2M$		$(C_5H_4)_2Fe$		$(C_5H_5)_2M$	$(C_5H_4)_2Fe$	
Ti	*a*	1.3 (s, 9)	6.07 (t, 2)	5.77 (t, 2)	4.35 (t, 2)	4.17 (t, 2)	5.94 (s, 5)	4.41 (t, 2)	4.08 (t, 2)
	b	1.27 (s, 9)	5.93 (t, 2)	5.43 (t, 2)	4.34 (t, 2)	4.11 (t, 2)	5.61 (s, 5)	4.32 (t, 2)	3.93 (t, 2)
Zr	*a*	1.30 (s, 9)	6.09 (t, 2)	5.78 (t, 2)	4.30 (t, 2)	3.98 (t, 2)	6.09 (s, 5)	4.39 (t, 2)	3.96 (t, 2)
	b	1.31 (s, 9)	6.00 (t, 2)	5.53 (t, 2)	4.33 (t, 2)	3.96 (t, 2)	not soluble		
Hf	*a*	1.35 (s, 9)	6.08 (t, 2)	5.78 (t, 2)	4.37 (t, 2)	3.95 (t, 2)	6.06 (s, 5)	4.44 (t, 2)	3.88 (t, 2)
	b	1.32 (s, 9)	5.95 (t, 2)	5.48 (t, 2)	4.40 (t, 2)	3.90 (t, 2)	5.41 (s, 5)	4.09 (t, 2)	3.48 (t, 2)

[a] In $CDCl_3$. [b] In C_6D_6.

These new compounds were isolated from the crude reaction residue by slow crystallization in toluene ($RCp = C_5H_5$) or in heptane ($RCp = t\text{-}BuC_5H_4$). Although the covalent radii of the transition metal used (Ti, 1.40 Å; Zr, 1.55 Å; Hf, 1.54 Å) are very similar to that of tin (1.55 Å), the reaction mixture never contained any dimeric or polymeric species.

The complexes isolated can be viewed as [1]ferrocenophanes or as metallacycles built from the metal center of a "bent" metallocene. The environment of the transition metal is consistent with four cyclopentadienyl ligands; two of them are σ-bonded, the two others being π-bonded (see X-ray structure). Metalla[1]ferrocenophanes react with HCl gas to give quantitatively an equimolar mixture of ferrocene and metallocene dichloride, as would be predicted. The stability toward water and oxygen, and consequently toward air, is related to metallocene structure. As previously reported for other complexes,[15] the greater the shielding provided by the cyclopentadienyl ligands, the better the stability to air. Thus, in spite of a strict exclusion of water and oxygen, metalla[1]ferrocenophanes (**1**) ($RCp = C_5H_5$; M = Zr, Hf) were rarely obtained as pure samples. ^1H NMR and mass spectra almost always show the presence of a small amount of oxygen-containing species in the reaction mixture further identified as μ-oxo complexes. The titanium-containing ferrocenophanes remain the most stable, and the $t\text{-}BuC_5H_4$ ligands allow the corresponding zirconium and hafnium solid complexes to be quickly handled in air.

In the presence of added water, complexes **1** afforded a mixture from which no definite products were identified. However, when exposed to air for a few hours, complexes **1** ($RCp = C_5H_5$; M = Zr, Hf) led to μ-oxo species in a good yield (reaction 2).

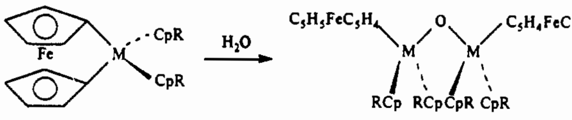

(2)

R = H; M = Zr, Hf

Spectroscopically speaking, the molecules of metalla[1]ferrocenophanes contain two distinct moieties. The ferrocene part is the most affected by the structural strains, and although there is no quantitative relation between [1]ferrocenophane molecular parameters and changes in spectroscopic parameters,[11,13] it has been shown that there is a correlation between the angle of the plane of the two cyclopentadienyl ligands (α in Figure 3) and the shift observed in the UV–visible spectrum of the ferrocene chromophore.[10,11]

Such a relationship does not appear in metalla[1]ferrocenophanes. For example, in spite of the bathochromic effect observed for complexes **1** ($RCp = t\text{-}BuC_5H_4$, M = Zr; $\lambda_{max} = 352$ nm) compared to free ferrocene ($\lambda_{max} = 325$ nm) the two cyclopentadienyl rings are not far from parallel as established by X-ray analysis.

^1H NMR results are reported on Table IV. The ferrocene protons are strongly influenced by the electronegativity of the bridging transition metal. They always appear as two triplets corresponding to two equivalent AA′BB′ spin systems with coupling constants of ca. 2 Hz. The most shielded triplet is the most influenced by the metal and is assigned to protons 2 and 4. These data can be compared to those observed for [2]ferrocenophanes,[16] in which the nature of the metal has a very slight impact on the chemical shift of the protons of the bonding metallocene moiety.

The ^{13}C NMR values for complexes **1** ($RCp = t\text{-}BuC_5H_4$) are reported in the Experimental Section. Data on [1]-

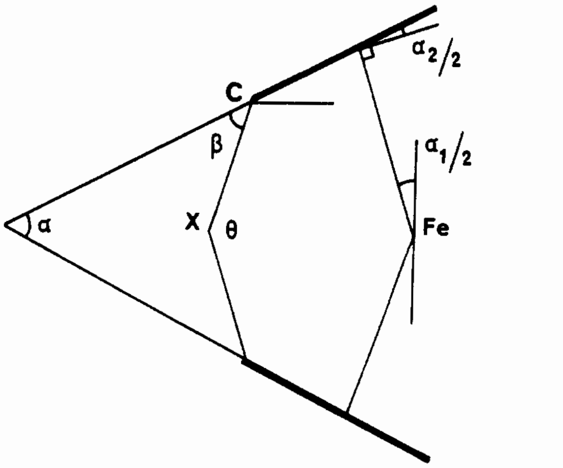

Figure 3. Distortions in ring-tilted ferrocenophanes describing angles α, β, and θ.

Table V. Selected Structural Data for $(t\text{-}BuC_5H_4)_2ZrL_2$ Compounds[a]

	$L_2 = (C_5H_4)_2Fe$[b]	L = Cl[c]	$L_2 = Se_2C_6H_4$[d]	
Zr–Cp′(c)	2.2549 (9)	2.217	2.236	2.209
Zr–Cp′(n)	2.251		2.230	2.207
Zr–C(5)	2.624 (2)	2.583	2.610	2.581
Zr–C(1)	2.583 (2)	2.547	2.587	2.527
Zr–C(2–4)	2.492–2.536	2.471–2.500	2.458–2.513	
C(2)–C(3)	1.381 (4)	1.383	1.394	1.381
other C–C	1.409–1.413	1.393–1.424	1.383–1.442	
Cp′(c)–Zr–Cp′(c)	125.31 (6)	128.6	129.9	
Cp′(b)–Zr–Cp′(n)	123.25	125.8	126.2	
diff	3.06	2.8	3.7	
C(4)···C(4′)	3.106 (3)	3.17	3.180	
C(3)···C(4′)	3.137 (3)		3.198	
C(2)···C(11)	3.150 (3)			
C(2)···C(12)	3.249 (4)		3.197	
C(1)···C(15′)	3.305 (4)			
C(1)···C(11′)	3.339 (3)			

[a] Distances in angstroms; angles in degrees. Cp′(n) refers to the projection of the metal atom onto the plane of the cyclopentadienyl ring. [b] This work. [c] Reference 17. [d] Reference 18.

---

(15) Cardin, D. J.; Lappert, M. F.; Raston, C. L. *Chemistry of organozirconium and -hafnium compounds*; Ellis Horwood, Ltd.: Chichester, England; Chapter 9.

(16) Rinehart, K. L.; Frerichs, A. K.; Kittle, P. A.; Westmann, L. F.; Gustafson, C. H.; Pruett, R. L.; McMahon, J. E. *J. Am. Chem. Soc.* **1960**, *82*, 4111.

Table VI. Selected Structural Data for [1]Ferrocenophanes $(C_5H_4)(R–C_5H_3)FeXR'$

	R, X, R′						
	H, PR′, C_6H_5[a]	H, PR′, *t*-Bu[a]	$CHN(CH_3)_2C_3H_7$, PR′, C_6H_5[a]	$CH(CH_3)N(CH_3)_2$, AsR′, C_6H_5[a]	H, SiR'_2, C_6H_5[b]	H, GeR'_2, C_6H_5[c]	H, ZrR'_2, *t*-BuC_5H_4[d]
mean Fe–Cp(n), Å	1.632 (3)	1.631 (2)	1.642 (2)	1.641 (1)	1.65	1.63	1.642 (2)
Fe···X, Å	2.774 (3)	2.763 (1)	2.764 (1)	2.8760 (3)	2.636 (5)	2.744 (3)	2.9621 (5)
X–C(11), Å	1.849 (5)	1.854 (3)	1.870 (2)	1.987 (2)	1.881 (11)	1.960 (10)	2.284 (2)
Cp(c)–Fe–Cp(c), deg	159.8	159.8	160.1	162.5	167.0	170.0	177.3
α, deg	26.9	27.1	27.0	22.9	19.2	16.6	6.0
α_1, deg	20.2	20.2	19.9	17.5	13.0	10.0	2.7
α_2, deg	6.7	6.9	7.1	5.4	6.2	6.6	3.3
β, deg	32.3	32.8	33.1	32.8	40.0	38.0	40.1
θ, deg	90.7	90.5	91.3	87.90	99.1	93.6	86.3
$2\beta + \alpha$, deg	91.5	92.7	93.2	88.5	99.2	92.6	86.2

[a] Reference 27. [b] Reference 25. [c] Reference 26. [d] This work.

ferrocenophanes[11,13] have shown that the C(11) and C(11′) resonances are shifted by 35–60 ppm upfield compared to the resonance position for a C(11) atom of nonbridged analogues. In contrast, the C(11) and C(11′) resonances of **1** were found at 150 and 180 ppm, downfield from other [1]ferrocenophanes. Thus, ^{13}C shifts are not a diagnostic of structural details.

Discussion of the X-ray Structure. The unit cell contains four molecules of $(t\text{-}BuC_5H_4)_2Zr(C_5H_4)_2Fe$ with C_5H_4-*t*-Bu designated as Cp′ and C_5H_4 as Cp hereunder. The molecule is made of two parts, $FeCp_2$ and $ZrCp'_2$. Each cyclopentadienyl Cp ring is also ligated to Zr by a σ-bond, so that it behaves as a σ,π-bridge.

The zirconium atom is pseudotetrahedrally surrounded by two π-bonded *tert*-butylcyclopentadienyl rings and by two σ-bonded C(11) and C(11′) carbon atoms belonging to the two cyclopentadienyl rings of the ferrocene moiety. In a sense, this compound may also be described as a [1]ferrocenophane for which the link between the two Cp's is the $ZrCp'_2$ moiety. The parameters of the coordination sphere of zirconium are close to those reported for Cp'_2ZrCl_2[17] and for $Cp'_2Zr(Se_2C_6H_4)$[18] (Table V). Both Cp′ rings are oriented around Zr in a such a way that the *tert*-butyl groups are turned toward the outside of the molecule, so that the steric interactions between the *tert*-butyl groups are minimized (Figure 2). The two cyclopentadienyl Cp′ rings make an angle of 122.25°, which is 3° less than those occurring in Cp'_2ZrCl_2 and in $Cp'_2Zr(Se_2C_6H_4)$.

The zirconium atom is not exactly equidistant from each cyclopentadienyl Cp′ carbon atom, and the largest distance corresponds to the carbon atom on which the *tert*-butyl group is attached; this is a feature already noted for Cp'_2ZrCl_2.[17]

Physical, theoretical, and structural data from several papers[19-24] related to heterobimetallic complexes have suggested the occurrence of a dative bond between an electron-rich and an electron-poor metal center. In our case, the Zr–Fe distance is found to be 2.9621 (5) Å.

This value is slightly longer than 2.926 (1) Å found for a Zr–Co compound $(C_5H_5)_2Co(\mu\text{-}CO)_2Zr(C_5(CH_3)_5)$[21] but shorter than the Ti–Cu distance found in $[(C_5H_5)_2Ti[SCH_2CH_2P(C_6H_5)_2]_2Cu]BF_4$[20] equal to 3.024 (1) Å. If we take into consideration the difference in the covalent radii between Fe^{II} (1.30 Å), Rh^{III} (1.32 Å), and Ru^{II} (1.33 Å), the experimental Zr–Fe distance appears to be longer than the Zr–Rh distance in $(C_5H_5)_2Zr[\mu\text{-}P(C_6H_5)_2]_2RhH(CO)P(C_6H_5)_3$[22] (2.980 (1) Å) and the Zr–Ru distance in $(C_5H_5)_2Zr[OC(CH_3)_3]Ru(C_5H_5)(CO)_2$[23] (2.910 (1) Å) or in $[(C_5H_5)_2Zr]Ru(CO)_2(C_5H_5)_2$[24] (2.943 (1) Å). We conclude that a weakened dative bond may occur between the electron-rich Fe atom and the electron-deficient Zr atom. This is probably influenced by the bonding between the Zr and the Cp rings which pushes the Zr away from Fe.

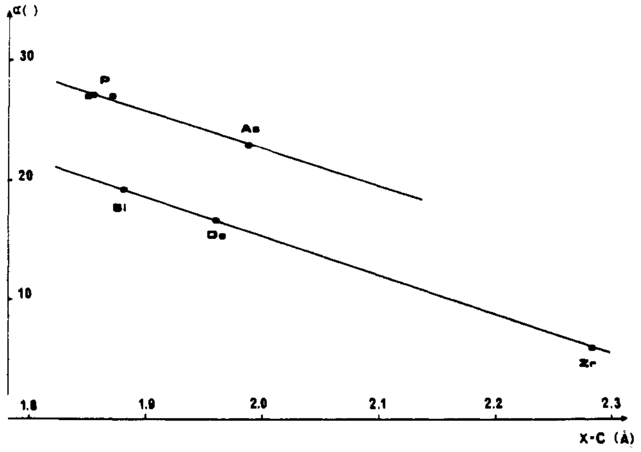

Figure 4. Variation of the angle α as a function of the distance X–C where X is the electron-poor metal atom in dinuclear X–Fe complexes.

In the ferrocene moiety both Cp rings take an eclipsed conformation such that the dihedral angle between the rings is 6°; this angle displays the rigidity of the iron–cyclopentadienyl orbital overlap. This eclipsed conformation is the result of the two σ-bonds to zirconium. The C(11)–C(12) and C(11)–C(15) intra-ring bonds (1.456 (3), 1.451 (3) Å) are significantly longer than the other ring C–C distances (1.408 (6), 1.415 (4), and 1.420 (4) Å; average 1.414 (5) Å).

Few [1]ferrocenophane structures have been published.[25-27] All of them exhibit strong distorsions, described by α, β, and θ angles shown in Figure 3[26] and Table VI. In the studied compound, the ferrocenyl geometry is noticeably different from those previously described. The α and θ angle values (6 and 86.3°) are the smallest observed in the series of seven [1]ferrocenophanes reported in Table VI, while the β angle is the largest. The β values may be gathered in two groups. For the four [1]ferrocenophanes in which the bridging atom belongs to group 15 (P, As), β ranges from 32.3 to 33.1°, with an average of 32.8°. For the three compounds in which the bridging atom belongs to group 4 (Zr) or 14 (Si, Ge), β is higher and ranges from 38 to 40.1°, with an average of 39.3°.

In Figure 4, α values are shown as a function of the X–C distance, X being the bridging atom. There is no obvious correlation, but both groups of values are found again. For group

---

(17) Howie, R. A.; McQuillan, G. P.; Thompson, D. W.; Lock, G. A. *J. Organomet. Chem.* **1986**, *303*, 213.

(18) Gautheron, B.; Tainturier, G.; Pouly, S.; Théobald, F.; Vivier, H.; Laarif, A. *Organometallics* **1984**, *3*, 1495.

(19) Holloway, C. E.; Walker, I. M.; Melnik, M. J. *J. Organomet. Chem.* **1987**, *321*, 143.

(20) White, G. S.; Stephan, D. W. *Inorg. Chem.* **1985**, *24*, 1499.

(21) Barger, P. T.; Bercaw, J. E. *J. Organomet. Chem.* **1980**, *201*, C39.

(22) Gelmini, L.; Stephan, D. W. *Organometallics* **1988**, *7*, 849.

(23) Casey, C. P.; Jordan, R. F.; Rheingold, A. L. *J. Am. Chem. Soc.* **1983**, *105*, 665.

(24) Casey, C. P.; Jordan, R. F.; Rheingold, A. L. *Organometallics* **1984**, *3*, 505.

(25) Stoeckli-Evans, H.; Osborne, A. G.; Whiteley, R. H. *Helv. Chim. Acta* **1976**, *59*, 2402.

(26) Stoeckli-Evans, H.; Osborne, A. G.; Whiteley, R. H. *J. Organomet. Chem.* **1980**, *194*, 91.

(27) Butler, I. R.; Cullen, W. R.; Einstein, F. W. B.; Rettig, S. J.; Willis, A. J. *Organometallics* **1983**, *2*, 128.

4 and 14 bridging atoms (Zr, Ge, Si), α varies nearly linearly. For group 15, only two values are plotted but the line joining these two points has the same slope.

If only elements belonging to the same period are considered, moving from group 14 to 15 (Si $\rightarrow$ P and Ge $\rightarrow$ As), variations of α, β, θ, and the X–Fe distance are as follows: $\Delta\alpha = 7°$, $\Delta\beta = -7°$, $\Delta\theta = -7°$, $\Delta d = 0.13$ Å. Smaller θ values for P and As compounds have been related to the lone pair.[27] The d distance increasing while the atomic radius slightly decreases may appear surprising. It might be explained by the repulsion of lone-pair electrons of the bridging atom with iron d electrons. For bridging atoms of a given period, the X–C and Cp–Fe distances remain fairly constant and consequently the d distance increase diminishes θ and β values as well as the ring leaning toward X; that is, α increases.

In contrast, the zirconium complex for which the d distance is the longest exhibits inverted variations: the β value is slightly increasing and the α value is highly decreasing. Consequently, the extreme values found for this case could be related to the long X–C distance, a result of the high atomic radius of the metal belonging to group 4.

It is interesting to note that the closest cyclopentadienyl–*tert*-butylcyclopentadienyl inter-ring distances are C(2)- - -C(11) = 3.150 (3) Å, C(2)- - -C(12) = 3.249 (4) Å on one side and C(1)- - -C(11′) = 3.339 (3) Å, C(1)- - -C(15′) = 3.305 (4) Å on the other side.

The structure is not exactly symmetrical, as shown in Figure 2. This figure also shows that the Cp′ rings are in a staggered situation. The shortest C- - -C distances between the two Cp′ rings are similar to values found for other compounds, 3.106 (3) Å for C(4)- - -C(4′) and 3.137 (3) Å for C(3)- - -C(4′). Corresponding distances are 3.17 Å for Cp'_2ZrCl_2[17] and 3.18 and 3.198 Å for $Cp'_2Zr(Se_2C_6H_4)$.[18] All cyclopentadienyl rings are planar within experimental error.

Supplementary Material Available: Tables of anisotropic thermal parameters (Table S1), fractional atomic coordinates (Table S2), bond lengths and angles (Table S3), equations of least-squares planes and distances from the plane (Table S4), and complete X-ray crystal data (Table S5) (5 pages); a table of observed and calculated structure factors (16 pages). Ordering information is given on any current masthead page.

Contribution from the Institut für Anorganische Chemie der Universität,
Egerlandstrasse 1, D-8520 Erlangen, Federal Republic of Germany

Transition-Metal Complexes with Sulfur Ligands. 50.[1] Sulfur Bond Cleavage in Organosulfur Ligands Induced by PPh$_3$/NO Substitution Reactions at [Ru(PPh$_3$)$_2$('L$_4$')] Centers ('L$_4$' = 1,2-Bis((2-mercaptophenyl)thio)ethanate(2–), 1,2-Bis((3,5-di-*tert*-butyl-2-mercaptophenyl)thio)ethanate(2–)). Synthesis and Reactions of Various (Vinylthio)arenethiolate and Related [Ru(NO)(Y)('L$_4$')] (Y = PPh$_3$, Cl) Complexes. X-ray Structure Analysis of Nitrosyl(triphenylphosphine)(1,2-benzenedithiolato)(1-(vinylthio)-2-benzenethiolato)ruthenium(III)

Dieter Sellmann,* Isabella Barth, Falk Knoch, and Matthias Moll

Received August 8, 1989

The ruthenium(II) complexes [Ru(PPh$_3$)$_2$(1,2-bis((2-mercaptophenyl)thio)ethanate(2–))], [Ru(PPh$_3$)$_2$('S$_4$')] (**1**), and [Ru(PPh$_3$)$_2$(1,2-bis((3,5-di-*tert*-butyl-2-mercaptophenyl)thio)ethanate(2–))], [Ru(PPh$_3$)$_2$('^{Bu}S$_4$')] (**2**), react with gaseous nitrogen monoxide. The substitution of one PPh$_3$ by NO is coupled with S–C bond cleavage of the 'S$_4$' and '^{Bu}S$_4$' ligands yielding the (vinylthio)arenethiolate complexes [Ru(NO)(PPh$_3$)(1,2-benzenedithiolate)(1-(vinylthio)-2-benzenethiolate)], [Ru(NO)(PPh$_3$)('S$_2$')('S$_2$'–CH=CH$_2$)] (**3**), and [Ru(NO)(PPh$_3$)(3,5-di-*tert*-butyl-1,2-benzenedithiolate)(1-(vinylthio)-3,5-di-*tert*-butyl-2-benzenethiolate)], [Ru(NO)(PPh$_3$)('^{Bu}S$_2$')('^{Bu}S$_2$'–CH=CH$_2$)] (**4**), respectively. A reaction mechanism via 19e$^-$ intermediates is suggested. Complex **3**·CH$_2$Cl$_2$ crystallizes in space group $P\bar{1}$ with $a = 1114.0$ (2) pm, $b = 1221.9$ (3) pm, $c = 1278.3$ (3) pm, $\alpha = 83.29$ (2)°, $\beta = 80.85$ (2)°, $\gamma = 76.91$ (2)°, $d_{calcd} = 1.56$ g/cm^3 ($Z = 2$), $R = 0.069$, and $R_w = 0.059$. In **3** the Ru center is pseudooctahedrally coordinated by nitrogen, phosphorus, and sulfur atoms. When complex **2** is reacted with NO$^+$ (NOPF$_6$), no S–C bond cleavage occurs and a complex forms being tentatively described as ionic [Ru(NO)(PPh$_3$)(1,2-bis((3,5-di-*tert*-butyl-2-mercaptophenyl)thio)ethanate(2–))](PF$_6$), [Ru(NO)(PPh$_3$)('^{Bu}S$_4$')](PF$_6$) (**5**). Neutral Ru(II) nitrosyl compounds with intact 'S$_4$'$^{2-}$ as well as '^{Bu}S$_4$'$^{2-}$ ligands are obtained when Ru(NO)Cl$_3$·H$_2$O is reacted with 'S$_4$'–Li$_2$ or '^{Bu}S$_4$'–Li$_2$, yielding [Ru(NO)(Cl)(1,2-bis((2-mercaptophenyl)thio)ethanate(2–))], [Ru(NO)(Cl)('S$_4$')] (**6**), and [Ru(NO)(Cl)(1,2-bis((3,5-di-*tert*-butyl-2-mercaptophenyl)thio)ethanate(2–))], [Ru(NO)(Cl)('^{Bu}S$_4$')] (**7**), respectively. All new complexes were characterized by spectroscopic means and elemental analyses.

Introduction

Transition-metal nitrosyl complexes are of interest as models for elementary steps of metal-catalyzed removal of nitric oxide from waste gases,[2] for key steps in the biological nitrate–ammonia conversion,[3] as catalysts in organic syntheses,[4] and as potential precursors for the synthesis of N$_2$ complexes.[5] One of the characteristic features of metal nitrosyl complexes is the dependence of the MNO angle upon the electronic configuration at the metal center, and angles from 120° up to nearly 180° are found.[5]

We are interested in metal nitrosyl complexes as chemical models for oxidoreductases, whose active centers consist of sulfur-coordinated transition metals[6] that can either activate or stabilize small molecules ranging from NO via hydroxylaminyl to NH$_3$.

In this context we recently found that 18e$^-$ NO complexes can be either reduced by one electron or by two electrons plus two protons. This is shown by the two couples [Fe(NO)('N$_H$S$_4$')]^n (n = 1+, 0) ('N$_H$S$_4$'$^{2-}$ = dianion of bis(2-((2-mercaptophenyl)-

---

[1] Part 49: Sellmann, D.; Käppler, O.; Knoch, F.; Moll, M. *Z. Naturforsch.*, in press.

[2] *Ullmanns Encyklopädie der technischen Chemie*, 4th ed.; Verlag Chemie: Weinheim, West Germany, 1981, Vol. 6.

[3] Hughes, M. N. In *The Inorganic Chemistry of Biological Processes*, 2nd ed.; John Wiley & Sons: New York, 1981.

[4] Pandey, K. K. *Coord. Chem. Rev.* **1983**, *51*, 69.

[5] McCleverty, J. A. *Chem. Rev.* **1979**, *79*, 53.

[6] Lowe, D. J.; Thorneley, R. N. F.; Smith, B. E. In *Metalloproteins Part 1: Metal Proteins with Redox Roles*; Harrison, P. M., Ed.; Verlag Chemie: Weinheim, West Germany, 1985.

0020-1669/90/1329-1822$02.50/0